UNIVERSIDADE FEDERAL DO CEARÁ

CAMPUS RUSSAS

GRADUAÇÃO EM ENGENHARIA CIVIL

VITORIA REBECA FERREIRA PINHEIRO

EVALUATION OF THE INFLUENCE OF CLIMATIC CHANGES ON THE DEGRADATION OF THE HISTORIC BUILDINGS

RUSSAS

2026

VITORIA REBECA FERREIRA PINHEIRO

EVALUATION OF THE INFLUENCE OF CLIMATIC CHANGES ON THE DEGRADATION OF THE HISTORIC BUILDINGS

Trabalho de Conclusão de Curso apresentado ao Curso de Graduação em Engenharia Civil da Universidade Federal do Ceará - Campus Russas, como requisito parcial para a obtenção do título de Bacharel em Engenharia Civil.
Orientador: Prof. Dr. Esequiel Mesquita

RUSSAS
2026

Dados Internacionais de Catalogação na Publicação
Universidade Federal do Ceará
Sistema de Bibliotecas
Gerada automaticamente pelo módulo Catalog, mediante os dados fornecidos pelo(a) autor(a)

P722e Pinheiro, Vitoria Rebeca Ferreira.
Evaluation of the influence of climatic changes on the degradation of the historic buildings / Vitoria Rebeca Ferreira Pinheiro. – 2026.
16 f. : il. color.

Trabalho de Conclusão de Curso (graduação) – Universidade Federal do Ceará, Campus de Russas, Curso de Curso de Engenharia Civil, Russas, 2026.
Orientação: Prof. Esequiel Mesquita.

1. Climatic changes. 2. Cultural heritage. 3. Degradation. 4. Pathology. 5. HBIM. I. Título.
CDD 620

Energy & Buildings 323 (2024) 114813

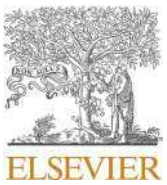

Contents lists available at ScienceDirect

Energy & Buildings

journal homepage: www.elsevier.com/locate/enb

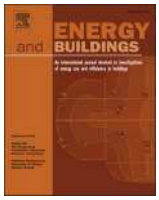

Evaluation of the influence of climatic changes on the degradation of the historic buildings

Vitoria R.F. Pinheiro [a], Rafael Fontenele [a], Allan Magalhães [a], Naggila Frota [b], Esequiel Mesquita [b,*]

[a] LAREB, Federal University of Ceara, Campus Russas, 62900-000 Russas, Brazil
[b] Department of Architecture and Urbanism and Design, Federal University of Ceara, Campus Benfica, 60020-181 Fortaleza, Brazil

ARTICLE INFO

Keywords:
Climatic changes
Cultural heritage
Degradation
Building pathology
HBIM

ABSTRACT

While climatic change has been a widely studied topic, its impact on cultural heritage degradation remains a gap to overcome. The environment can contribute to the degradation of historic buildings and materials decay, especially temperature and humidity. So, characterizing the micro-climates of a landmark zone and understanding the influence of the recovery layers, building disposition, and street characteristics on environmental parameters are the first steps to investigating resilience strategies for heritage conservation and micro-climates. Thus, this paper presents a new approach to assess the influence of climatic warming on historic building degradation, combining multiscale experimental data and numerical modeling. The environmental parameters of the historic center of Aracati downtown, such as concentration of CO_2, relative humidity, temperature, and air condition, were characterized and used together with urban volumetry to discuss the influence of on the urban microclimate and relate the data to the physical degradation of cultural heritage. An uncrewed aerial vehicle was used to register the volumetry of the historic center, and the data was used to simulate the wind conditions. Following this, numerical analysis was used to investigate the rising damp and thermal tension distributions under temperature variation over the years (from 2023 to 2100). The methodology's applicability was demonstrated in recurrence with the Nosso Senhor do Bonfim Church, one of the most representative heritage constructions from Aracati downtown. Finally, the new methodology contributed to understanding how urban volumetry contributes to the climatic conditions of a historic area and demonstrates that the increase of the temperature can significantly affect the rising damps and the development of stress tension.

1. Introduction

The impact of climate change on the built environment emerges as one of the most significant challenges of the 21st century [1,2]. This phenomenon is primarily characterized by an increase in the frequency and intensity of extreme weather events and natural disasters, such as a substantial rise in the number of extremely hot days, droughts, sea-level rise, floods, and intense precipitation, projected for the near future [3–6].

Anthropogenic actions are widely recognized as one of the main causes of climate change, resulting in a global warming of about 1.0 °C compared to pre-industrial levels in 1850–1900 [4]. This warming is projected to reach 1.5 °C between 2030 and 2052 if the current rate continues [4]. Changes in global temperature patterns and extreme temperature values drastically affect societies, the environment, and ecosystems [7,8]. This threat extends to historical heritage, including buildings and monuments, which face significant long-term preservation risks. Recent studies [9,10] shows that climate change is worsening the degradation processes of historic buildings and archaeological sites worldwide. Thus, urban warming represents an additional threat to the preservation of these constructions, amplifying the challenges faced by historical structures and monuments.

In this line, unplanned growth of the cities has led to altering land use and covers layers and the energy balance of cities, intensifying the Urban Heat Island (UHI) effect, which increases temperatures in urbanized areas due to high building density, asphalt paving, strangle streets and human activities. Thus, UHI impacts urban comfort and climate management, as widely discussed in the scientific literature [11–13]. The surface-level version of UHI, known as Surface Urban Heat Island (SUHI), refers to the increase in surface temperature in urban

* Corresponding author.
E-mail address: emesquita@ufc.br (E. Mesquita).

https://doi.org/10.1016/j.enbuild.2024.114813
Received 16 May 2024; Received in revised form 20 August 2024; Accepted 14 September 2024
Available online 17 September 2024

areas compared to their rural surroundings, documented in various cities worldwide, such as Athens [14], Sydney [15], Milan [16], Singapore [17] cities in California [18], significantly impacting urban systems, affecting the urban anthroposphere, hydrosphere, biosphere, and atmosphere [9]. The evaluation of UHI magnitude reveals that its intensity can reach up to 5 °C and even exceed 8 °C [19].

UHI is related to the increase in the frequency, duration, and intensity of heat waves [20]. UHI indices during heat waves in the Baltimore-Washington metropolitan area are significantly higher than in other locations [21], substantially affecting urban centers and densely populated areas, including cultural heritage sites, making them less habitable [22]. This increases the global demand for electricity for heating, ventilation, and air conditioning, can negatively affecting heritage [23,24]. Varas-Muriel and Fort [25] highlight the delicate balance between the natural microclimate and heritage conservation, with constant disturbances intensifying the damage [24,26–33]. To address climate challenges, the scientific community has been developing mitigation and adaptation measures [34–37].

Implementing new materials is an effective strategy to mitigate the urban warming. Cool roofs and pavements optimize radiative exchanges with solar and environmental radiation [38–40], phase change materials store and release solar thermal energy [41], and evapotranspiration and vegetation, like green roofs, improve urban comfort [42–45]. Combining these strategies can significantly reduce the average air temperature by 2.7 °C and the peak temperature by 3.5 °C [45]. Assessing the vulnerability of historic areas to heat waves is crucial and is being addressed globally [46].

Despite efforts to mitigate climate change, these strategies must be reviewed in historic centers due to cultural conservation restrictions [31]. Architectural modifications must respect the cultural values of historic zones [47], which were built to meet the needs of specific eras. Due to these factors, the effects of climate change are intensified in the preservation of cultural heritage, requiring resilience strategies. The reuse of historical structures is common, but internal improvements are limited by architectural restrictions [48], necessitating continuous monitoring [49,50]. Therefore, it is crucial to understand how climate warming impacts the degradation of historical heritage, varying in different geographical and cultural contexts. The interaction between climate change, urbanization, and heritage management is complex and underexplored, hindering effective strategies, especially in tropical climates.

This study assumes that the climate crisis is already underway and emphasizes the importance of mitigating the effects of climate change on historical buildings, addressing gaps in research on heritage degradation. It offers an interdisciplinary approach involving climatology, archaeology, architecture, and heritage management, providing insights for adaptation policies essential to preserving cultural legacy.

Presenting an innovative multiscale experimental monitoring methodology focused on measuring the influence of climatic changes on historic building degradation. The methodology was demonstrated by application in two scales, the urban scale approached the limits of Aracati historic center and use equipment and sensors for data collection, such as the Temtop® M2000 and the Flir® E5-XT thermal camera, a 2 km route was mapped in areas with different types of paving and tree cover to capture temperature peaks. It characterizes the environmental parameters of the historic center of Aracati, discussing the influence of urban volumetry on the microclimate and relating these data to the physical degradation of historical heritage.

Them, the building scale using the Church of Nosso Senhor do Bonfim in Aracati, a heritage site classified by the Instituto do Patrimônio Histórico e Artístico Nacional (IPHAN) in 2001. The aerial and the Leica BLK360 laser scanner generated the point cloud. In the laboratory, software like WUFI 2D, Flow Design, and Ansys were used for simulations, analyzing degradation caused by temperature, wind action, and mechanical stresses. This technique combines environmental monitoring and climate impact analysis on materials, providing data for predictive analysis of heritage wear and supporting guidelines to prevent environmental degradation. The approach presented has reproducibility potential in historic centers, increasing their resilience to extreme climatic events.

2. Historic Center of Aracati and the Nosso Senhor do Bonfim Church

Aracati is a coastal city in northeastern Brazil, 160 Km away from the capital of Ceara State, Fortaleza, and 507.35 Km from the equator line, as presented in Fig. 1. The Historic Center (HC) of Aracati is a historical area of the town composed of streets and architectural monuments from the 18th, 19th, and 20th centuries, as well as the surrounding polygonal area, which encircles the strict preservation area and is also regulated by a series of restrictions regarding physical interventions. Its construction dates to the 18th century, the era of the Cattle Cycle, the 19th century, the commercial and cotton cycle, and the 20th century, the industrial cycle. The architectural ensemble became recognized as a national heritage, and the IPHAN listed it in April 2001.

The Bonfim Church is one of the oldest constructions in Aracati, beginning in 1772 and completed in 1774. The church is 405 m distant from the Jaguaribe River, and over the centuries the building has been affected by floods and has undergone many changes, but it still maintains its original facade. The church structure is naturally affected by the mechanism of rising damp [51]. The church's altar is carved in wood and houses richly detailed Baroque paintings and sculptures from the 18th century in white and gold colors. In Aracati, the summer is short, hot, and dry, while the winter is brief, warm, and with precipitation. The weather is oppressive throughout the year, with winds reaching 24 km/h and nearly overcast skies. The temperature typically ranges from 23 °C to 35 °C throughout the year. The historic center exhibits significant temperature variations, highlighting the critical point around the heritage site.

3. Methodology

3.1. Environmental micro-urban measurements

The first part of proposed method aims to characterize the environmental parameters of the historic center of Aracati; to discuss the influence of urban volumetrics on the urban microclimate, and to correlate the data with the physical degradation of cultural heritage. Data collection was facilitated trough wearable sensors, which continuously gathered information on air temperature (Ta) and relative humidity (UR) throughout the campaign. Figs. 2 and 8 illustrates the step-by-step of the proposed methodology: Stage 1) environmental data collection; Stage 2) digital survey and point cloud acquisition; Stage 3) multiparameter numerical analysis; Stage 4) microclimate characterization and historic masonries degradation behavior; and Stage 5) indication of the most critical area in surround of N. S. do Bomfim Church. The environmental data collection was carried out on November 11th, 2023 (summer in the Southern Hemisphere), during which the weather forecast indicated a minimum temperature of 23 °C and a maximum of 36 °C, with a wind speed of approximately 24 km/h from the east and relative humidity ranging between 59 % and 94 %.

The state of Ceará is located globally very close to the equator (South Latitude: 4°46′30″; Longitude 37°14′45″), so it does not have a large temperature range. Santos et al (2010) analyzed the historical series of average temperatures in the northeast region of Brazil from 1961 to 2007 using data from the National Meteorological Institute (INMET) and came to the conclusion that "average air temperatures are found to vary between 22 and 25 °C". In order to find more recent information on the temperature range, the authors of this study systematized data from the official weather station located in Jaguaruana, far away 30 km from Aracati. According to the climatological normal for the years 1991–2020 (Fig. 3), there is a maximum temperature range of 12° and a minimum of

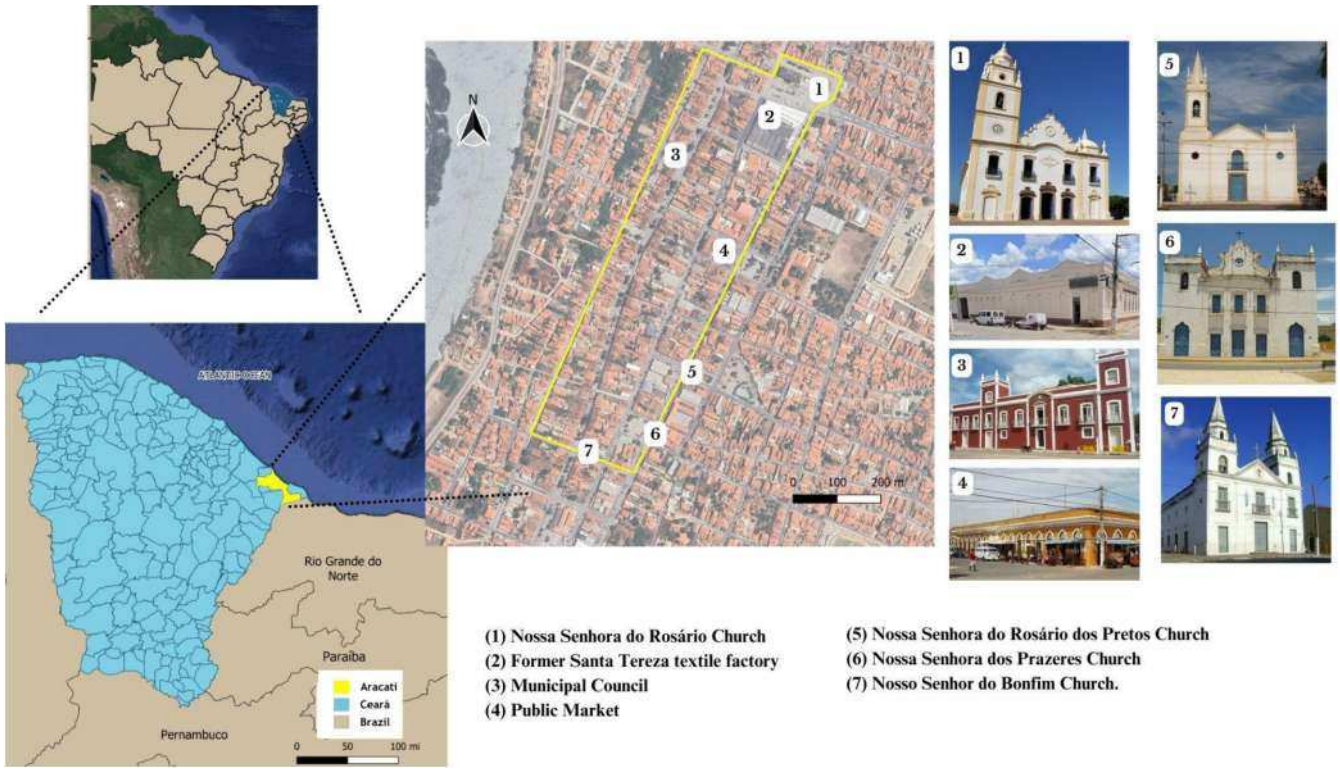

Fig. 1. Location of Aracati downtown in the Ceará State map.

8°. Therefore, there is no significant thermal variation throughout the year which requires extensive data collection, since the data collected would have very close values.

The monitoring equipment was used to perform a multiparameter micro-urban environment analysis from a pedestrian perspective. An air quality monitor, Temtop® M2000, a portable device capable of measuring PM2.5, PM10, carbon dioxide, formaldehyde, temperature, and humidity, was employed to record the data. The recording device provides accurate real-time readings, allowing immediate observations as environmental conditions change. Environmental data was collected every 1 min and automatically stored. In addition, a Flir® E5-XT infrared thermography imaging camera was used to characterize the street temperature. Flir® E5-XT has a high-precision infrared detector with 19,200 (160 × 120) pixels and an extended temperature range from −20 °C to 400 °C. Its capabilities enable the identification of points or areas where temperature deviates from a predefined or known pattern. A GPS was used to register each location along the route. By correlating the environmental information with GPS, it was possible to identify potential heat locations, facilitating proactive intervention and analysis.

The selected route encompasses a variety of pavement types, building heights, facade materials, and vegetation concentrations, generating several different microclimates within the city and incorporating significant historical landmarks, such as churches listed by IPHAN (Fig. 1 and Fig. 2). Therefore, conducting an analysis to understand how the microclimate near these landmarks may contribute to their degradation is relevant.

The route, as shown in Fig. 2, had a length of approximately 2,000 m, and climate data were collected at each 1 min interval, automatically generated and stored by the Temtop® device. The entire route was conducted by walking (Fig. 4), as the length of the monitoring route selected allowed for completing the perimeter in less than 1 h. The route was performed three times a day: at 6:00 a.m., during the peak of minimum temperature under solar incidence, at the maximum temperature peak, at 2:00p.m., and at the time with the average temperature, where solar radiation is expected to be negligible, at 6:00p.m. (Fig. 5). The time recorded routes corresponded to 43, 45, and 42 min at 6:00 a.m., 2:00p.m., and 6:00p.m., respectively.

The availability of GPS data facilitates the integration of data into Geographic Information Systems (GIS). The QGIS platform was essential in enabling the generation of custom route images according to selected parameters, using a comprehensive range of colors. More specifically, the data plotted on aerial images in QGIS depict air temperature variation in the monitored urban environment through a color palette of 13 points, where the obtained data adjusts according to pre-established parameters.

The thermographic images were time-stamped and linked to GPS data to ensure accurate localization. The emissivity has been set at 0.85 to represent the typical thermal behavior of the built environment, considering that the properties of the analyzed materials have an emissivity ranging from 0.80 to 0.95, with a target-to-camera distance of up to 20 m. The infrared pictures were processed using FLIR® Tools software for enhanced image quality and details.

The surface temperature records allowed reliable analyses with these settings, highlighting discernible differences within an image due to unique elements such as vegetation, pavement type, and shaded areas along the same path. To emphasize this objective, the range of surface temperature palettes chosen remains consistent for all corresponding infrared images of the same monitoring route during specific time intervals: 20 °C to 40 °C at 6 in the morning, 20 °C to 60 °C at 2 in the afternoon, and 20 °C to 40 °C at 6 in the evening.

In Fig. 6, there is the spatialization of three different criteria that can influence the temperature, including the type of road surfacing, the height of the buildings, and the presence of vegetation. All this information was collected by mapping the elements in the aerial image by point cloud. About the type of paving, it was noticed a more significant presence of stone cobblestone, followed by concrete interlocking blocks and a slight stretch of asphalt. It is worth noting that the colors of these materials vary from lighter for the first two to darker for the last. As for the height of the buildings, sensible variation in the volume built was noted, with buildings varying between 1 and 2 floors. However, the

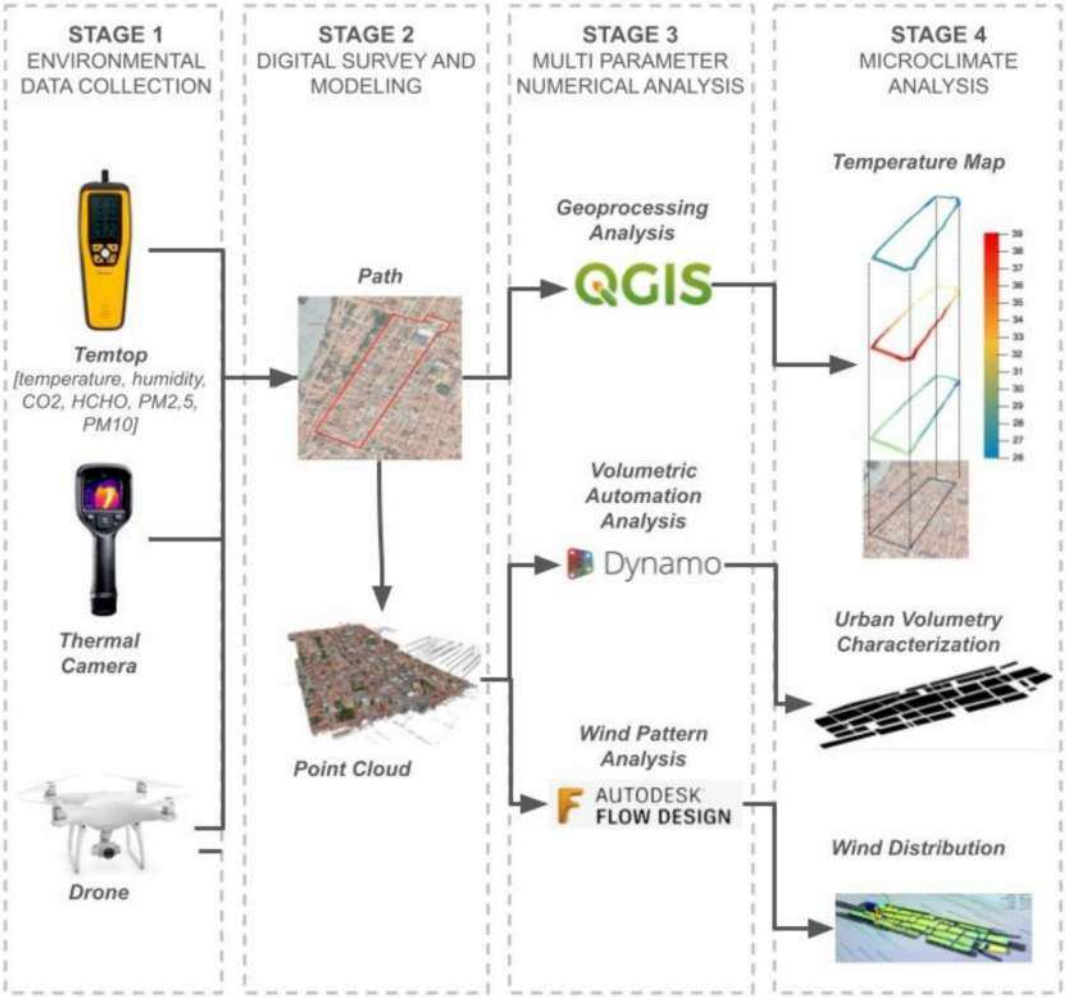

Fig. 2. Scheme of the part one of methodology for evaluation degradation of historic buildings influenced by climate change.

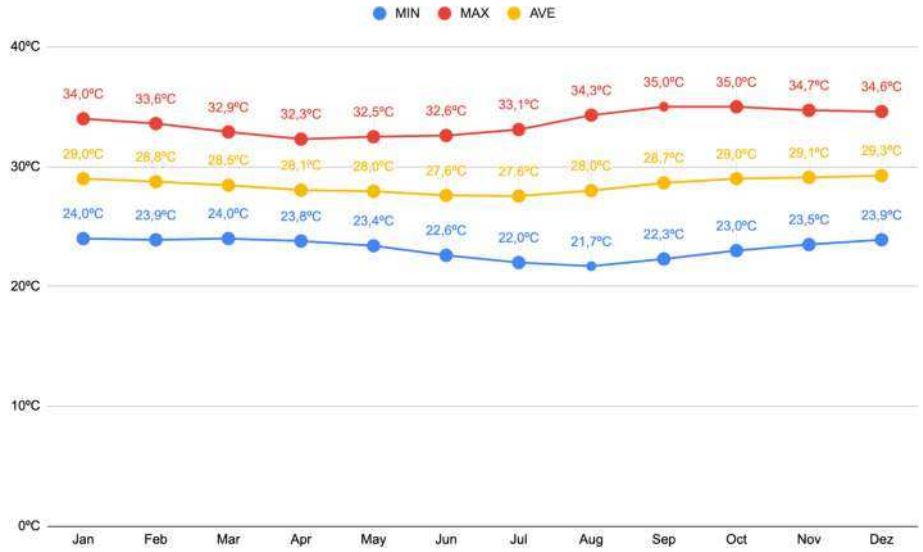

Fig. 3. Comparative graph showing the maximum, average and mean values of Brazil's Climate Normals between 1991 and 2020. . Scheme of the methodology for evaluation degradation of historic buildings influenced by climate change.
Source: National Institute of Meteorology. Available at: https://portal.inmet.gov.br/normais

Fig. 4. Environmental data recording along the Aracati historic center perimeter.

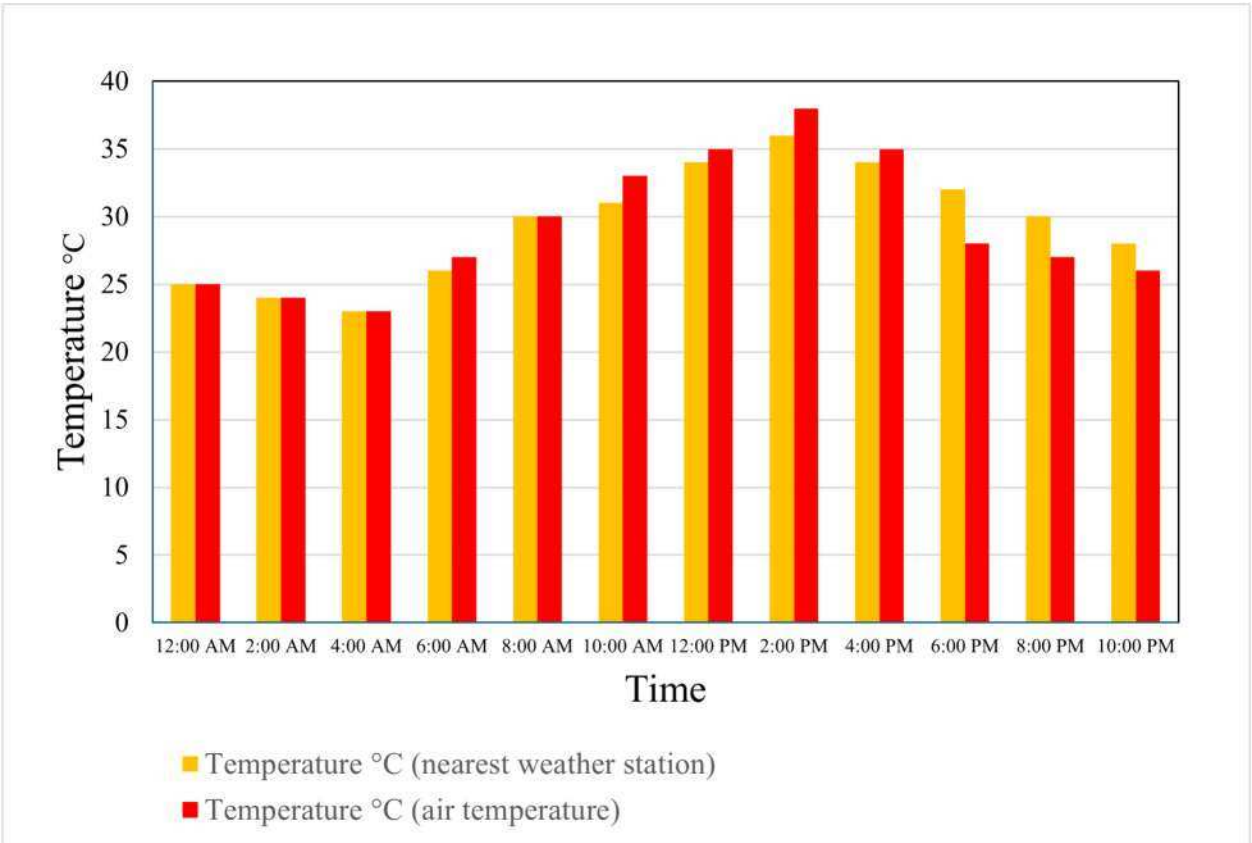

Fig. 5. Average temperature of a typical day at Aracati downtown.

areas without buildings, here considered free squares, stand out along the route. Concerning the presence of vegetation, it was possible to observe small portions of vegetation distributed along the roadbed. The most significant mass of vegetation was found near of the northwest stretch within empty plots of land.

3.2. Geomatic processing

An unnamed aerial vehicle (UAV), as presented in, was used to generate a point cloud (Fig. 2 and Fig. 7) of the Aracati historic center to conduct volumetrics of the streets. Additionally, a point cloud of the streets and the churches was recorded using the Leika® BLK Laser Scanner to obtain measurements of the church and provide some

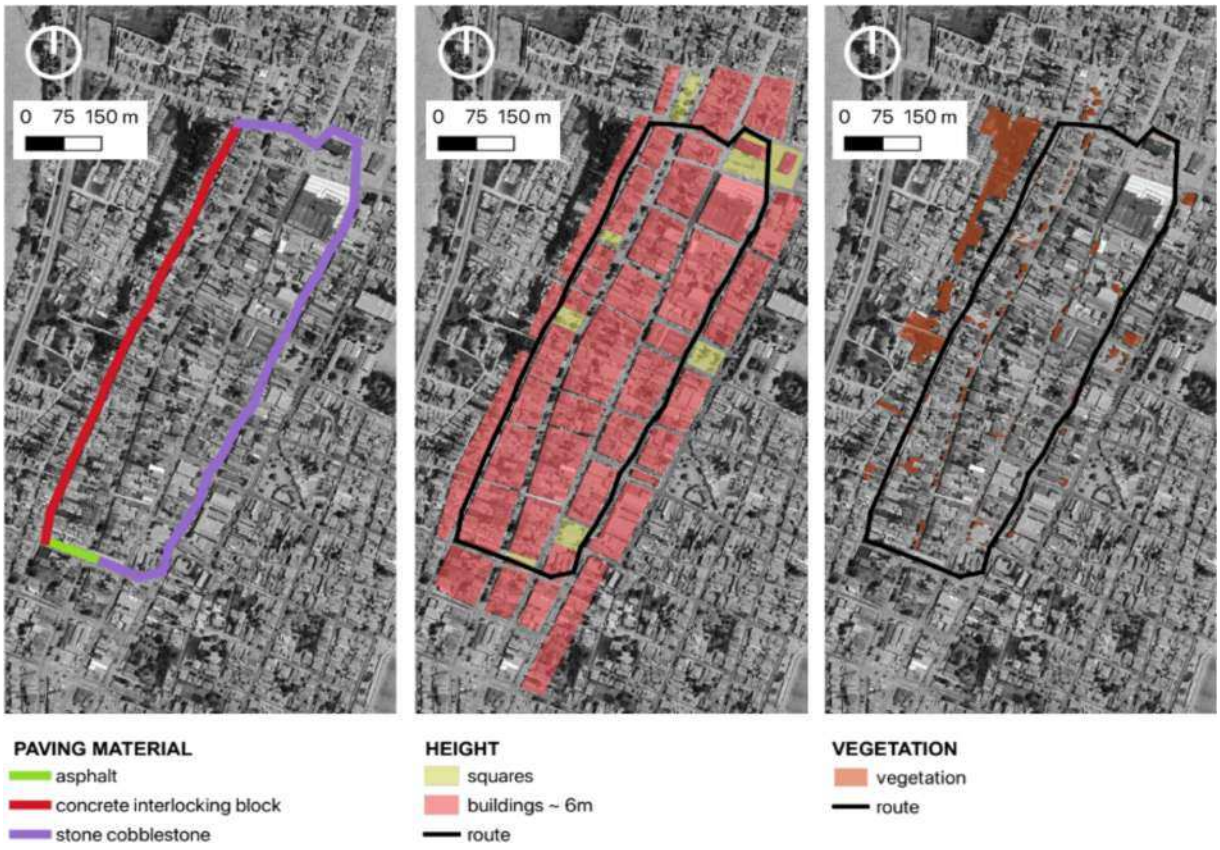

Fig. 6. Micro-urban environmental aspects of Aracati downtown.

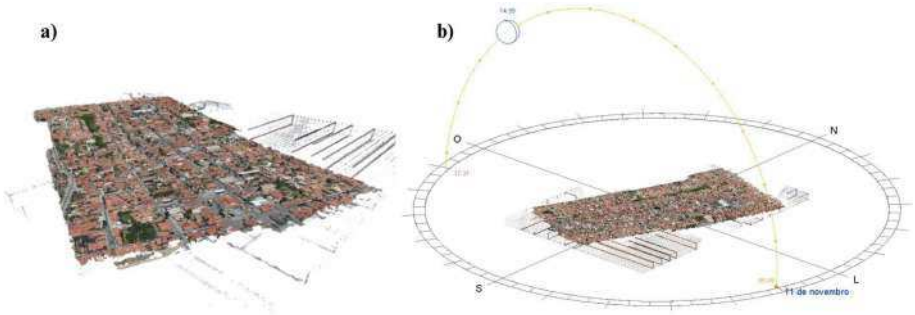

Fig. 7. Point cloud generated by UAV capture: a) point cloud of Aracati downtown and b) solar analysis.

adjustments in the volumetry used to solar analysis (Fig. 7). Subsequently, the historic center volumetry was automatically transferred through Dynamo® to the Flow Design® software for the wind velocity pattern analysis.

After observing the data obtained with the first phase of the method (environmental micro-urban measurements and geomatic processing), it was possible to define the areas most affected by high temperatures and then choose the significant building as the spatial cut-out used in the second phase described below.

3.3. *Physical modeling and evaluation of the historic building degradation*

The second part of the method aims to carry out a structural analysis of a relevant historic building according to future climate change scenarios. For this purpose, the N. S. do Bomfim Church was used as the object of study, according to the results of the first part of the method. The Global Climate Model called HadGEM2-ES, made available by the Ministry of Science, Technology and Innovation (2020) was used as the simulation model. Th is model was chosen because it is a downscaled regional approximation. We chose to apply the temperature changes predicted in the report to two scenarios, for the year 2050 and then for the year 2100. The second part of the method followed the same steps as the first part, but used other devices to collect data and other software for the simulation (Fig. 8).

Regarding the thickness and variations of the historic masonries, depending on the measurements and construction phases over time, the configuration of the masonry structure can vary considerably within the same building, as observed in the case of the Church of Nosso Senhor do Bonfim (Araújo et al., 2020). With dimensions of 2.00 m × 1.20 m, the walls feature a core of clay bricks coated with a layer of lime mortar.

The influences of climatic changes on the degradation of historic masonries were simulated considering rising damp, capillarity profile and moisture content under variations of temperature and relative humidity over the years. To simulate this model, a dimension of 2.00 m ×

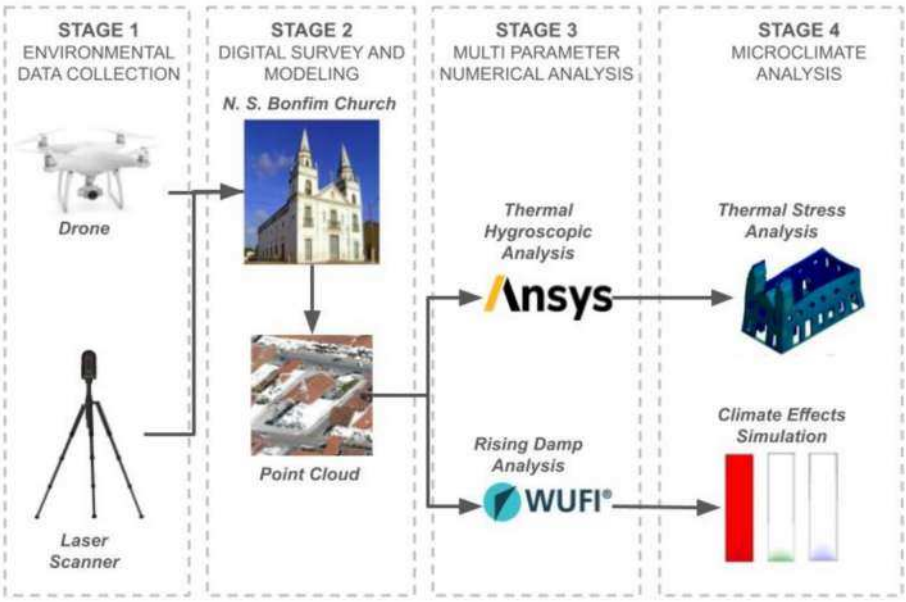

Fig. 8. Scheme of the part two of methodology for evaluation degradation of historic buildings influenced by climate change.

0.57 m was adopted to study the presence of rising damp in the church masonry, considering future predictions for the years 2050 and 2100. The physical and mechanical properties of the masonries of Nosso Senhor do Bonfim used for the numerical analysis were obtained by previous work of the authors [52]. The complete description of the materials is presented by Table 1.

The models of historical walls were numerically simulated using WUFI 2D software, version 4.5, which employs a computational approach to analyze the thermal and hygroscopic performance of insulation and masonry systems in buildings. These analyses allow the simulation of heat and moisture transport in materials in a two-dimensional analysis, considering material properties and climatic conditions to evaluate changes in moisture content. The WUFI 2D considers non-linear equations proposed by Kunzel [53], as presented by Equations (1) and (2). For the simulation, the time frame considered in this study was 4,320 h, equivalent to a half-year.

$$\frac{dH}{dT}\frac{\partial T}{\partial t} = \nabla(\lambda \nabla T) + h_v \nabla(\delta_p \nabla(\phi p_{sat})) \tag{1}$$

Table 1
Physical properties of the historic masonries of the Nosso Senhor do Bonfim Church used for numerical simulation on WUFI.

Bricks			Mortar		
Properties	Value	Unity	Properties	Value	Unity
Water absorption	10.9	%	Natural moisture content	1.64	%
Natural moisture content	1.8	%	Density	1600	kg/m^3
Compressive strength	16.5	N/mm^2	Porosity	30	%
Porosity	21.2	%	Specific heat	850	J/kg.K
Density	1950	kg/m^3	Thermal conductivity	0.7	W/m.K
Specific heat	850	J/kg.K	Water vapor diffusion coefficient	7	–
Thermal conductivity	0.6	W/m.K	Proportion (binder: sand)	1:6	–
Water vapor diffusion coefficient	10	–	Binder	Limestone	–

$$\frac{dw}{d\varnothing}\frac{\partial \varnothing}{\partial t} = \nabla(D_\varnothing \nabla \varnothing + \delta_p \nabla(\phi p_{sat})) \tag{2}$$

where:

$\frac{dH}{dT}$ is the heat storage capacity of the wet materials ($J/(m^3.K)$).
$\frac{dw}{d\varnothing}$ is the moisture storage capacity of wet material (kg/m^3).
λ is the thermal conductivity of wet material ($W/(m.K)$).
h_v is the enthalpy of water evaporation (J/kg).
$D_\varnothing$ is the liquid conduction coefficient ($kg/(m.s)$).
δ_p is the water vapor permeability of the material ($kg/(m.s.Pa)$).
T is the temperature ($^\circ C$).
w is the moisture content of the material (kg/m^3).
$\varnothing$ is the relative humidity (−).
p_{sat} is the water vapor saturation pressure (Pa).

The simulations were based on IPCC [54] projections for current temperature in the years 2050 and 2100, while relative humidity was calculated as an average due to minimal variation. The average temperature considered was 38 °C for 2050 years and 43 °C for 2100, respectively, with an average relative humidity of 60 %. These data indicate that the region where the Church is located experiences high temperatures and high relative humidity throughout the year. The computational evaluation was performed by adopting thermal conduction and moisture migration simultaneously, presenting their data in two ways: in 2D format or through graphs. The 2D visualization offers a clear and interactive representation of the results, allowing tracking of changes in temperature, relative humidity, capillarity, and others over time. This visualization allowed visualization of the results based on object position, which can be easily adjusted, and enables legend modification for a more flexible analysis.

To analyze how temperature variation influences the degradation of historical heritage, a complementary analysis with finite element simulations to evaluate mechanical stresses resulting from thermal variations was carried out using Ansys® software, version 2023 R1, which allows greater precision and versatility in structural analysis. In order to optimize the computational resources, the church was reproduced based on the scanner survey. Additionally, a structural state stress analysis was also performed.

Referring to the construction of the 3D numerical model, given the required level of precision for the simulation, it became feasible to approximate the ceramic and mortar elements to a homogeneous

material using macromodeling techniques. The modeling was carried out in Revit and imported into Ansys®, where a 0.2x0.2 m mesh was defined for the entire 3D element. The "Soft" option was chosen as it provides greater mesh refinement, especially in corners and regions with "critical" geometry, where more detailed analysis is required, resulting in 52,043 elements and 293,508 nodes.

In the thermal stress analysis, Ansys® software provides predefined values for the initial conditions of the materials, with a temperature of 20 °C and a relative humidity of 80 %. However, these values were adjusted to reflect the real conditions of the study, as the entire church facade faces west, experiencing abrupt temperature variations over 24 h, which further intensifies wear over the years. The lowest and highest temperatures captured by the thermal camera were added to identify the variation range, along with Poisson's ratio and Young's modulus, to allow stress load demands on the wall.

For the material properties, the existing literature was used to find the usual data for this study. Table 2 summarizes the mechanical properties adopted in the church's numerical model. Thus, the Specific Weight (w) and Compressive Strength (fc) were obtained through the average parameters found in [55]. The Modulus of Elasticity (E) and Tensile Strength (ft) were obtained from [56]. Finally, Poisson's ratio was defined based on the works [57–59], which was 0.20. With the data entered, transient analyses of temperature, von-Mises stresses, and structural deformations were performed, as the primary aim of the project was to analyze the behavior of the historical heritage over time and with variations in the predefined parameters.

4. Results

Analyzing the microclimate characterization of the Aracati historic center, as presented by Figs. 9, 10 and 11, and considering that the temperature varies by 2 °C degrees, the temperature color spectrum did not vary significantly enough to change color at night; it remained stable between 26 °C and 28 °C degrees. In addition, Figs. 9, 10 and 11 present critical points that require special attention to preserve the heritage in the surroundings, especially during the afternoon and morning.

Also, it is possible to observe that between paths 1 and 2, there was a milder temperature during the morning hours than in the other passages. This is attributed to the considerable wind circulation (Fig. 12), as it features shaded pavement areas during that time and also wide roads with stone cobblestone pavement. During the afternoon, something similar occurs during the first half of the stretch; however, during the second half, wind circulation becomes more complex, preventing temperature exchange. However, between paths 2 and 3, it is possible to note significant differences in temperatures on the morning (28 °C to 30 °C) and afternoon (32 °C to 36 °C) thermal maps. This can be attributed to a subtle narrowing of the roads, almost complete absence of greenery, higher solar exposure during the day, and hindered air circulation by surrounding buildings.

The analysis of wind circulation (Fig. 12) allowed to observe the wind influence on specific points, such as point 3 of the thermal images, identified as the hottest section of the route (39 °C to 40 °C). The surrounding buildings distort air masses, resulting in the absence of wind circulation at that point. Furthermore, the lack of green areas and wind circulation significantly contributes to the heating of this section compared to other highlighted points. While 39 between 43 (90,69 %) of the buildings of the Aracati Historic Center present 1 or 2-story, the presence of 3 to 6-story buildings in line works as an obstacle to the winding course. This scenario contributes to generating areas with poor ventilation, as it can be noted that a major part of the streets is not well-ventilated, especially the transversal streets.

Between paths 3 and 4, the morning and afternoon thermal maps show a slight temperature variation (39 °C to 37 °C). This can be attributed to a change in pavement layer from stone cobblestone to asphalt and an even more significant road narrowing. In the afternoon, three significant temperature variations (39 °C to 35 °C) are visible between paths 4 and 5. These decrease progressively due to various factors, including wider roads, pavement made of cement interlocking blocks, less solar exposure, and a gradual increase in green areas.

In paths 5 and 6, during the afternoon map, another significant decrease in temperature (35 °C to 33 °C) can be observed. This is because the temperature gets closer to the green area, and air circulation occurs more quickly. Another interesting aspect to analyze here is paths 6 and 7, where green areas nearby and broader streets with cement interlocking blocks and stone cobblestone pavements result in milder climatic conditions than in other sections (33 °C to 31 °C). This is due to the shade and evapotranspiration the trees provide, which favor the local microclimate. In paths 7 and 8, it is not possible to identify a very significant difference in either of the maps; the temperature remains practically constant between one point and another and stable between 31 °C and 32 °C.

Temperature and humidity are generally correlated, but usually inversely, meaning that when the temperature increases, the relative humidity decreases, and vice versa. This occurs because water molecules have more kinetic energy when the temperature is high, leading to an increased evaporation rate from liquid surfaces and vegetation. In Fig. 13 and Fig. 14, it is presented the variation of temperature and relative humidity associated with the complete route.

With the mapping of the environmental microclimate of the Aracati historic center, it was observed that all levels of CO_2 are lower in the afternoon than at other times (Fig. 14e). This is because, at 2p.m., there is practically no urban movement, as it is the peak of heat during the day. The increase in temperature during the afternoon can contribute to better air circulation and the dissipation of atmospheric pollutants. Even though the CO_2 concentration measurements are lower than 660 ppm, point as the safety limit to the human daily exposition, the values of 520 ppm are considerably high for a small downtown. That behavior reflects the absence of materials or vegetation able to capture or store the CO_2 from the atmosphere. However, CO_2 levels (Fig. 14e) tend to increase during the night due to heightened urban activity and a drop in temperature. As the day winds down, urban activities such as vehicular traffic and heating systems continue to emit carbon dioxide. Additionally, the decrease in temperature overnight can contribute to stagnant air and the accumulation of atmospheric pollutants, including CO_2. This combination of factors results in higher levels of carbon dioxide during nighttime hours, posing additional challenges for air quality in urban areas.

The PM2.5 particulate matter mapping (Fig. 14c) indicates that it is at highly critical and unhealthy levels, and the entire population may face serious risks of respiratory and cardiovascular diseases in the near future (if it is not facing that now). There is an increased risk of premature deaths among individuals in sensitive groups. The PM10 particulate mapping (Fig. 14d) indicates acceptable concentrations without adverse health effects.

Following the projections outlined in the IPCC's VI report [4], temperature forecasts for 2050 and 2100 indicate a maximum increase under the most adverse global scenario, starting from 2023, of 1.4 °C and 3.6 °C, respectively. Conversely, the minimum increase under the most favorable global scenario is projected to be 0.4 °C and 0.3 °C, respectively. Based on IPCC's data [4], the climatic prediction to 2050

Table 2
Physical properties of the historic masonries of the Nosso Senhor do Bonfim Church used for numerical simulation on Ansys.

Mecanic properties	Magnitude
E (GPa)	1.70
w (kN/m^3)	18.00
f_c (MPa)	3.20
f_t	0.16
ν	0.20

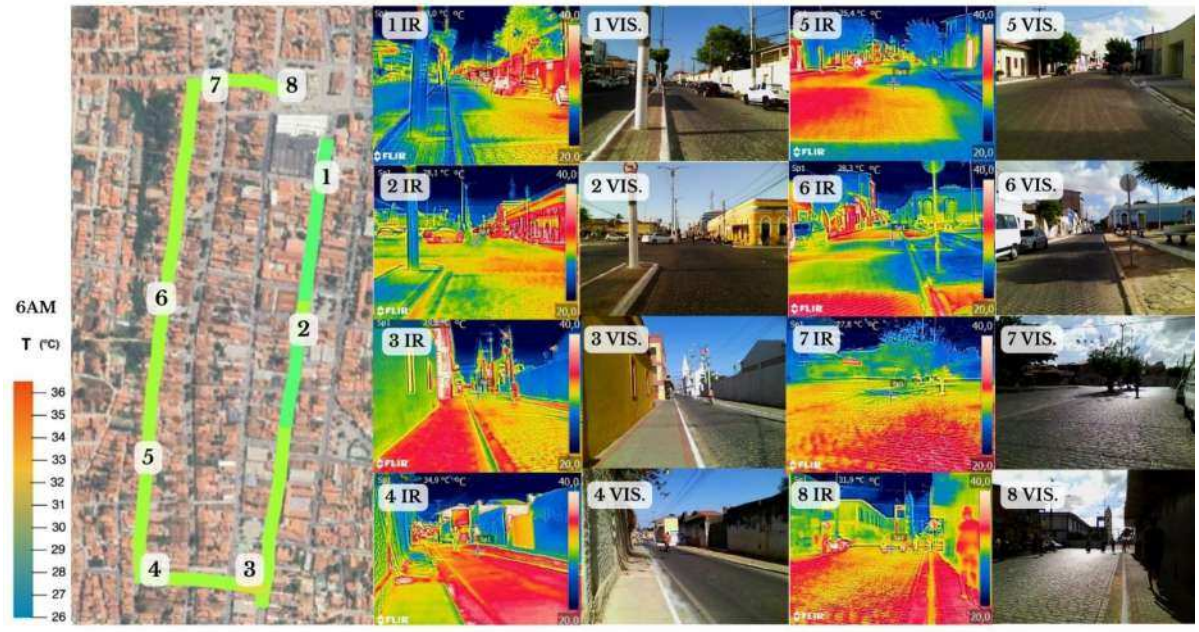

Fig. 9. Micro-climate characterization of Aracati historic center: temperature and infrared thermography records along the route at 6 a.m.

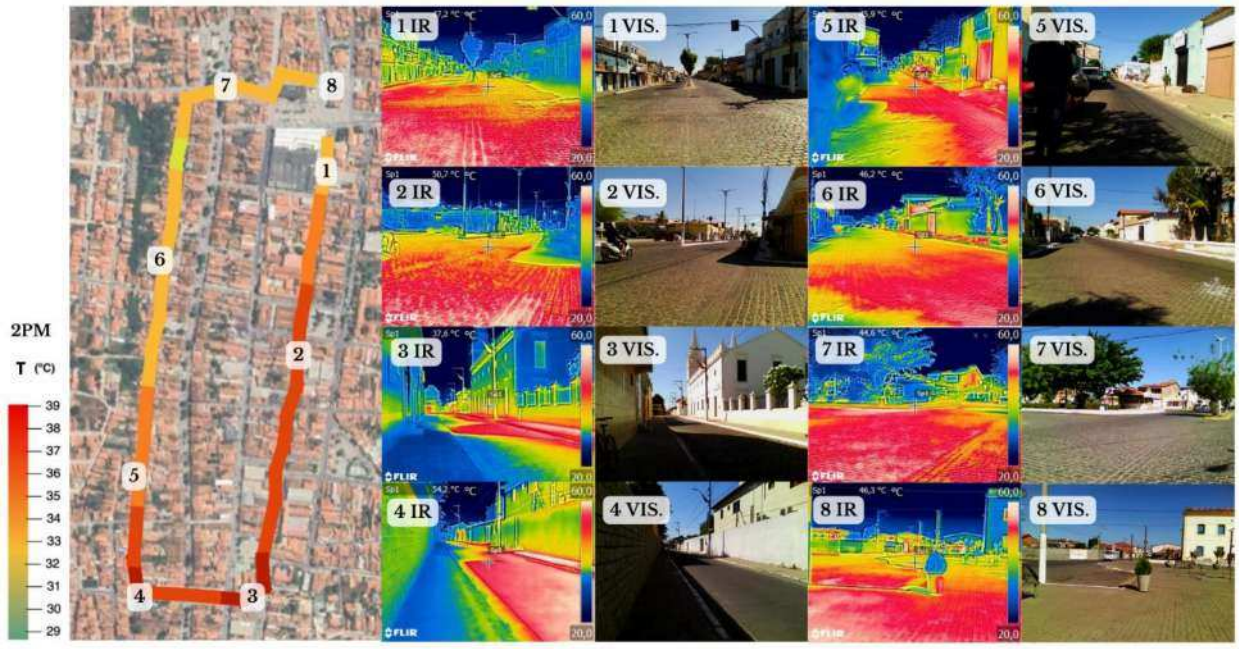

Fig. 10. Micro-climate characterization of Aracati historic center: temperature and infrared thermography records along the route at 2p.m.

and 2100 to Aracati historic center was obtained through a simple sum between the 2023 value and the projection value, as presented by Fig. 15. Report projections was based in WGIII, a large number of global modelled emissions pathways were assessed, of which 1202 pathways were categorized based on their projected global warming over the 21st century, with categories ranging from pathways that limit warming to 1.5 °C with more than 50 % likelihood with no or limited overshoot to pathways that exceed 4 °C. Methods to project global warming associated with the modelled pathways were updated to ensure consistency with the AR6 WGI assessment of the climate system response.

As temperatures rise, the lifecycle of structures in the region accelerates due to various factors, one of which is very prevalent: rising damp caused by capillarity, mainly due to dissolved salts in the water. With the increase in temperature, the rate of water evaporation from the wall increases, leaving only the salts lodged in the pores of the materials, resulting in a decrease in diameter and consequently further increasing capillarity.

In terms of microclimate control, the results indicate the importance of expanding the vegetation cover and replacing asphalt roads to mitigate the effects of high temperatures in the coming years. The other elements that influence the microclimate, such as the width of the roads and the material of the facades, are fundamental elements for preserving Aracati's historic site and are protected by legislation against severe modifications. Therefore, these elements maintain the same aspects over

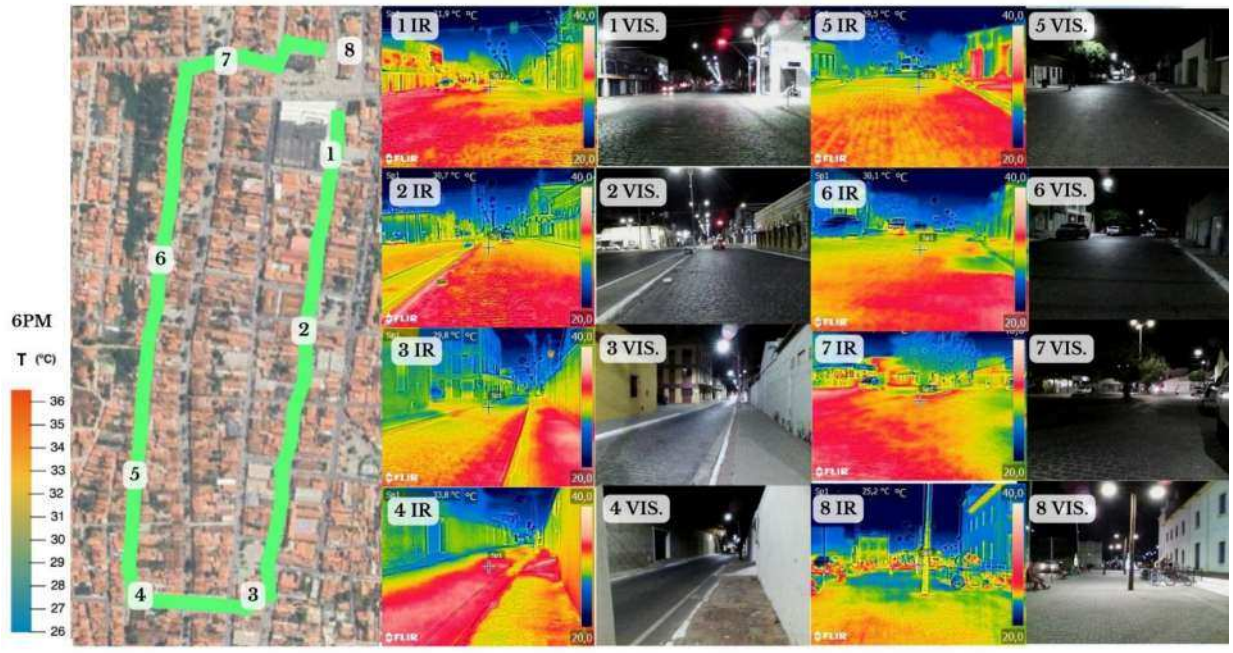

Fig. 11. Micro-climate characterization of Aracati historic center: temperature and infrared thermography records along the route at 6p.m.

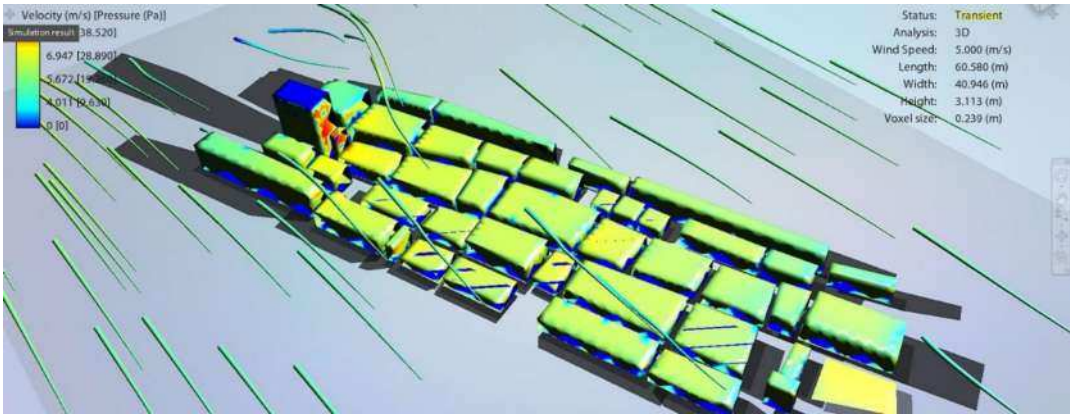

Fig. 12. Wind direction and velocity pattern analysis.

the years, causing the same type of influence on the microclimate.

The degradation level of historical heritage due to climate change versus the urban heat island (UHI) effect is multifaceted and interdependent. Climate change exacerbates extreme weather events, such as increased temperatures, altered precipitation patterns, and more frequent and intense heatwaves, which accelerate the deterioration of historical structures by causing thermal expansion, material fatigue, and increased biological growth. Conversely, the UHI effect, a localized climate phenomenon resulting from urbanization, intensifies heat stress on buildings through higher ambient temperatures and reduced cooling at night. This exacerbates the degradation processes initiated by climate change, leading to a compounded impact on historical heritage. The study reveals that while climate change sets the broader stage for heritage vulnerability, the UHI effect acts as a localized amplifier of these impacts, significantly accelerating material degradation and structural wear. Thus, addressing both global climate change and localized urban planning is essential for developing comprehensive conservation strategies to preserve historical heritage.

The thermal simulations of the church walls obtained using Ansys software (Fig. 16.a, b, and c), demonstrate an increase in the church's covering layers, with maximum values ranging from 40.56 °C in 2023 to 45.84 °C in 2050 and 51.12 °C in 2100. These values were calculated based on measurements taken using a thermal camera, with additional data from the IPCC's VI Assessment Report and predictions from the HadGEM2-ES global model incorporated into the temperatures captured in 2023. In the case of thermal movements, it is important to consider not only the temperature range but also the duration of time over which these changes occur, as different materials have varying response times to thermal alterations, especially thermal shocks, where sudden changes can result in high stresses and material degradation [60,61]. Thermal shocks occur daily; however, the climate crisis is exacerbating the range of daily temperature fluctuations. The average temperature variation of the building's walls between minimum and maximum values is 10.75 °C in 2023, followed by an increase to 16.12 °C in 2050 and 21.50 °C in 2100. The increase in the differences between minimum and maximum temperatures influences the thermal movements of the coverings, indicating the formation of cracks due to fatigue caused by thermal effects. The results demonstrate a significant difference in stresses over the years, as presented in Fig. 16, clearly indicating an approximate 400 % increase in thermal deformation compared to the initial observation

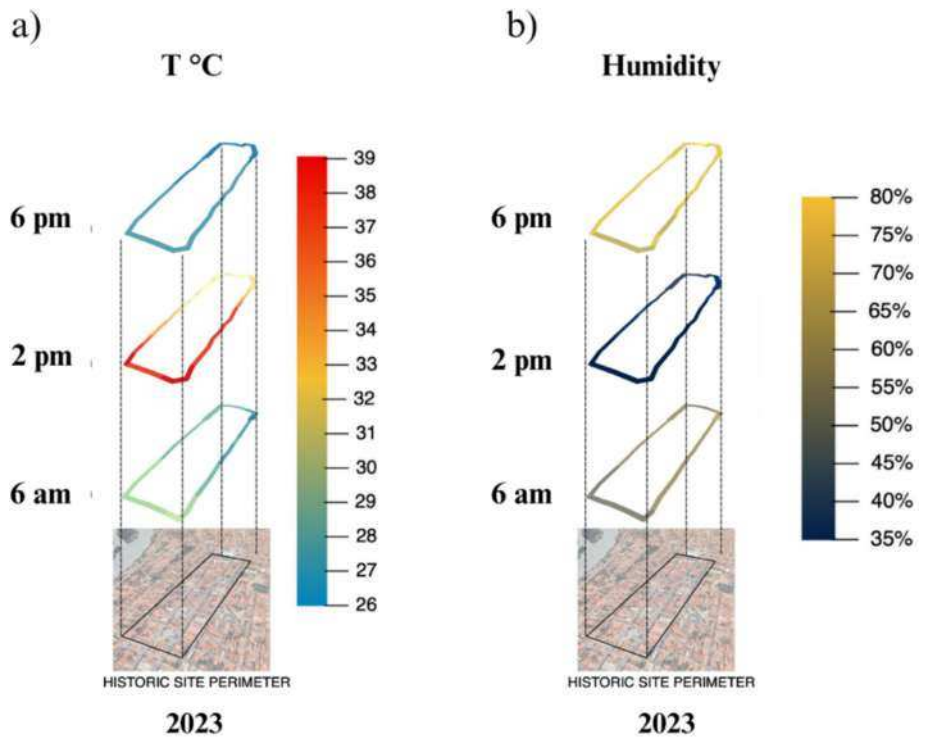

Fig. 13. Environmental characterization of Aracati downtown: a) temperature and b) humidity collected along the route throughout the day.

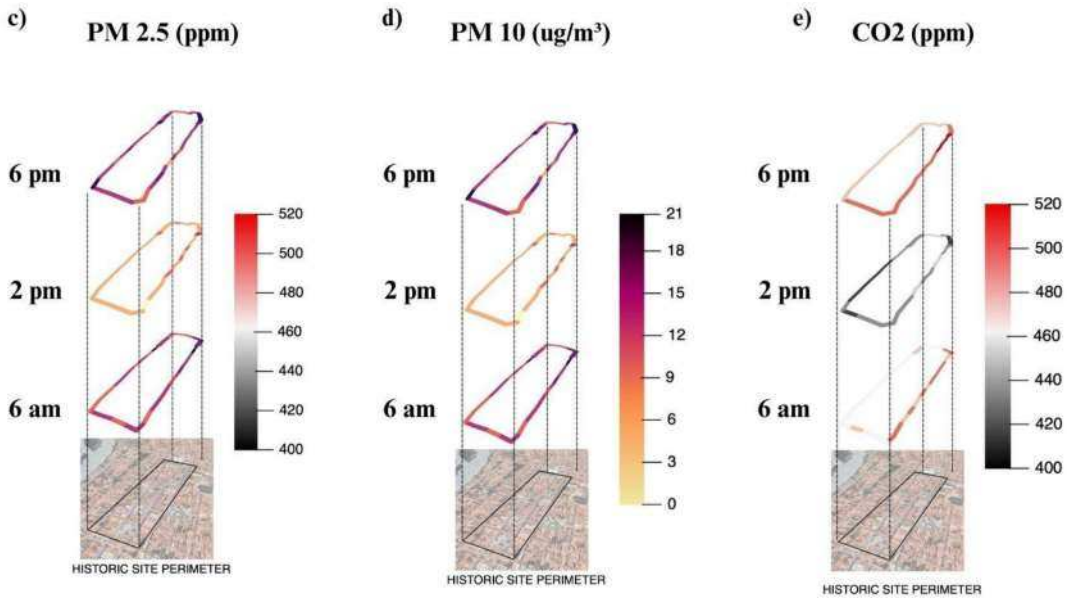

Fig. 14. Environmental characterization of Aracati downtown: c) PM2,5; d) PM10, and e) CO2 along the route throughout the day.

year (Fig. 16.g, h, and i), leading to considerable degradation. These results are consistent with previous studies (reference two studies). The von-Mises stress simulation (Fig. 16.d, e, and f) highlighted the structural stress points, where values range from 1.4814 × 10^-12 MPa in 2023 to 1.544 MPa in 2050, reaching a maximum of 3.067 MPa in 2100, while the stress resistance limit of the masonry is around 0.16 MPa [57,61], indicating a widespread scenario of cracks in the masonry facades. Additionally, the historical building is not only affected by stresses caused by thermal variations; those caused by rising moisture with the presence of salts are also quite significant, given that Aracati is a coastal area with intense salt air, and the deposition of these salts in the soil is a reality.

Temperature and its variation can affect negatively the fatigue behavior of mortars and similar materials. The low values of Von-Mises stress are developed when the values of the environmental temperature are near of 25 °C, while the maximum values of temperature are developed when the values of the environment are higher than 39 °C. The values up to the limit of resistance of mortars indicate the cracks formations over the coating layers. While works that investigate the effect of temperature on the thermal stress of historic buildings are

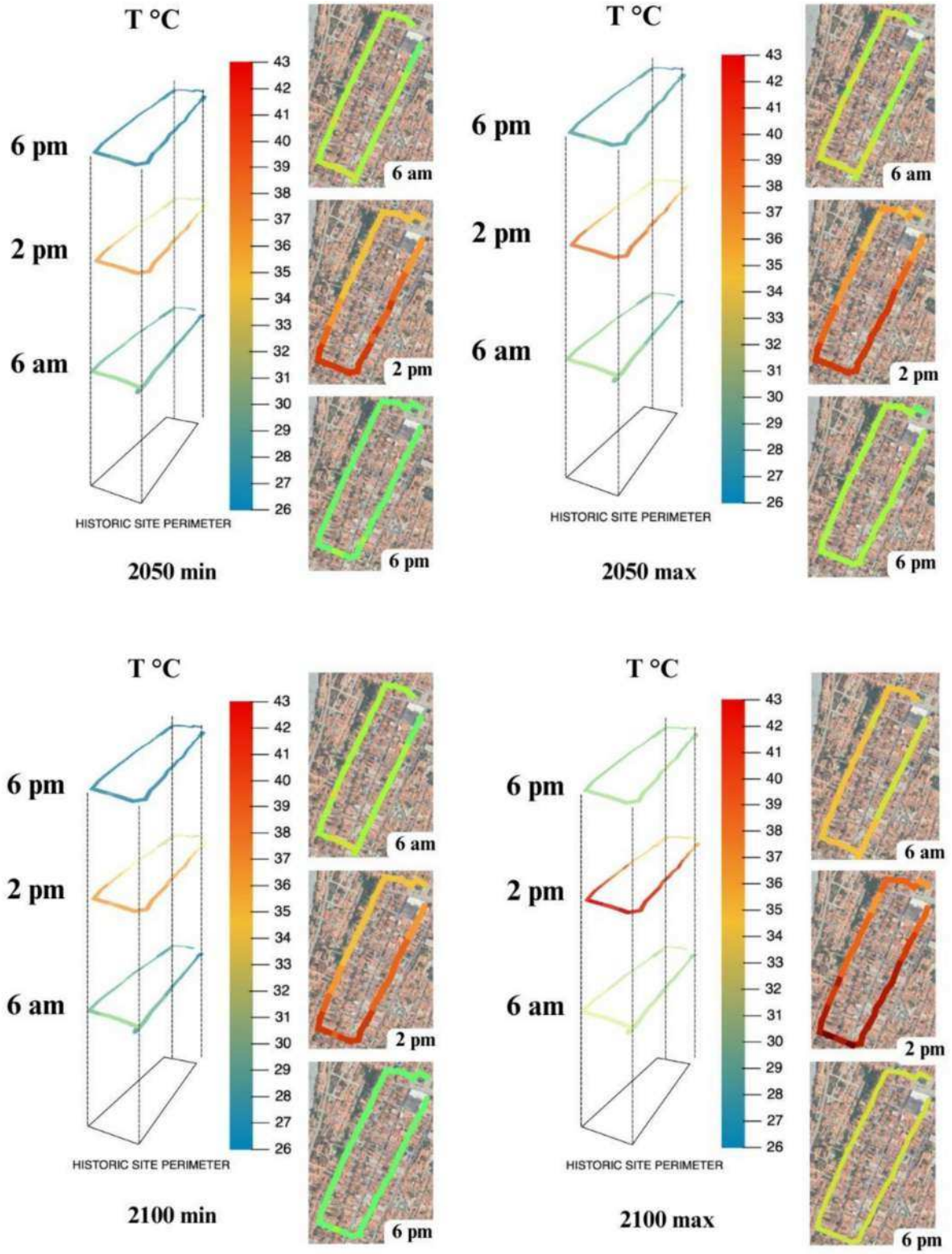

Fig. 15. Prediction of the maximum and minimum temperatures of Aracati downtown to 2050 and 2100.

rarely reported in the literature, similar works with mortars and concrete presented similar behavior than the results founded in this paper [62–66].

Following, the results indicate higher stress demands at the bottom part of the masonry, caused by rising damp, accentuated by the capillarity present in salty water, abundant in the coastal region of Aracati. As temperatures rise (Fig. 17a) and the increase of moisture content (Fig. 17b), the water is easily evaporated, leaving only the salts trapped in the building materials' pores, reducing pore diameter. Consequently, this causes a constant increase in capillarity (Fig. 17c) and rising damp (Fig. 17d), resulting in amplified wear and deterioration. The detailed behavior of the rising damp is presented by Fig. 18 where it is possible to identify the total water content increases from 0.37 kg/m^3 in 2023, to 0.45 kg/m^3 in 2050, and finally the failure of the masonry due to the

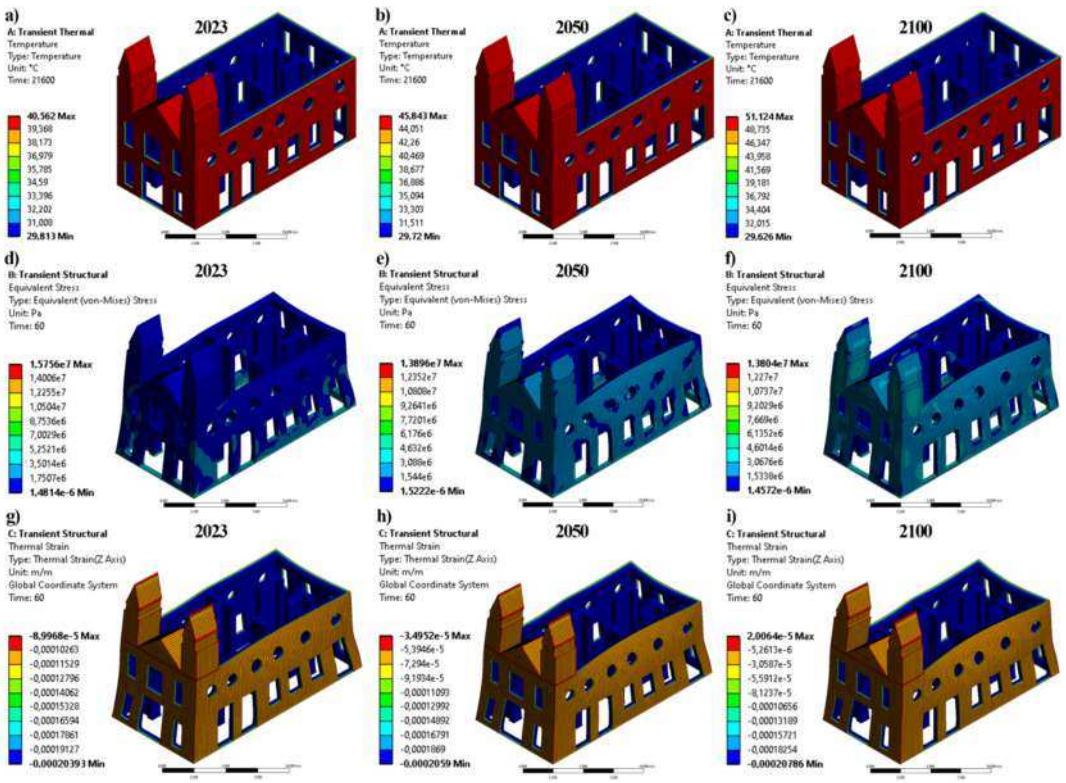

Fig. 16. Simulation of the transient thermal, transient structural stress and thermal strain of the historic masonries of the Nosso Senhor do Bonfim Church.

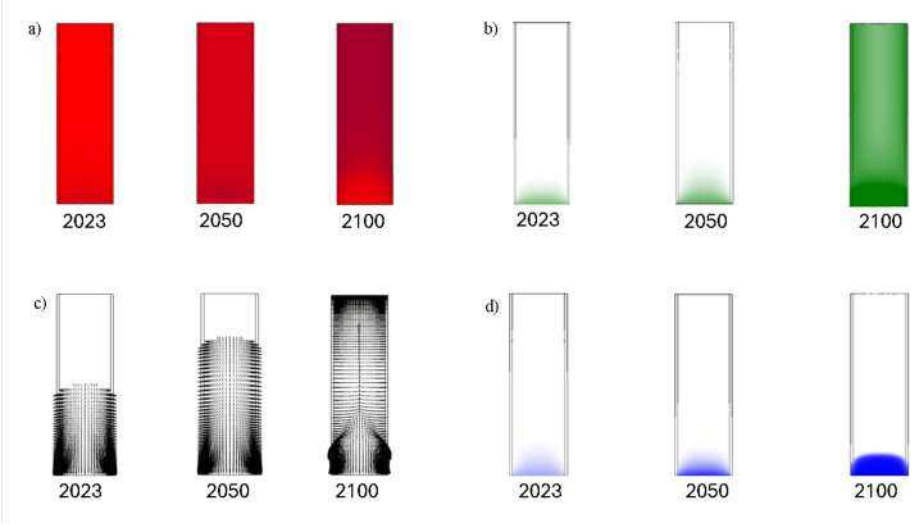

Fig. 17. Effect of the climatic change on the degradation of historic masonries: a) thermal behavior, b) moisture content, c) capillarity, and d) rising damping by WUFI 2D in 2023, 2050, and 2100.

capillarity advance and the crack emergence.

While rising damp can be influenced by the temperature increase, the solar exposition and the thermal stress also plays a relevant role to the historic masonries degradation. The increasing in the temperature accelerates the capillarity effect and the water transport through the masonry pores. The water also affects the lime dissolution, decreasing the mortar cohesion and facilitating the cracks emergence and the mechanical failure, contributing this way to structure degradation.

5. Conclusions

The present article introduced an innovative methodology for quantitatively investigating how climate changes and even the microclimate surrounding buildings contribute to heritage degradation. The method consists of aerial and terrestrial digital scanning, multiparameter environmental characterization, and numerical simulations. The methodology demonstrated to be able to cover relevant issues on degradation of the historic buildings and able to identify critical areas in the historic center more susceptible to warming. The complete characterization of the urban microclimate also provided reliable information

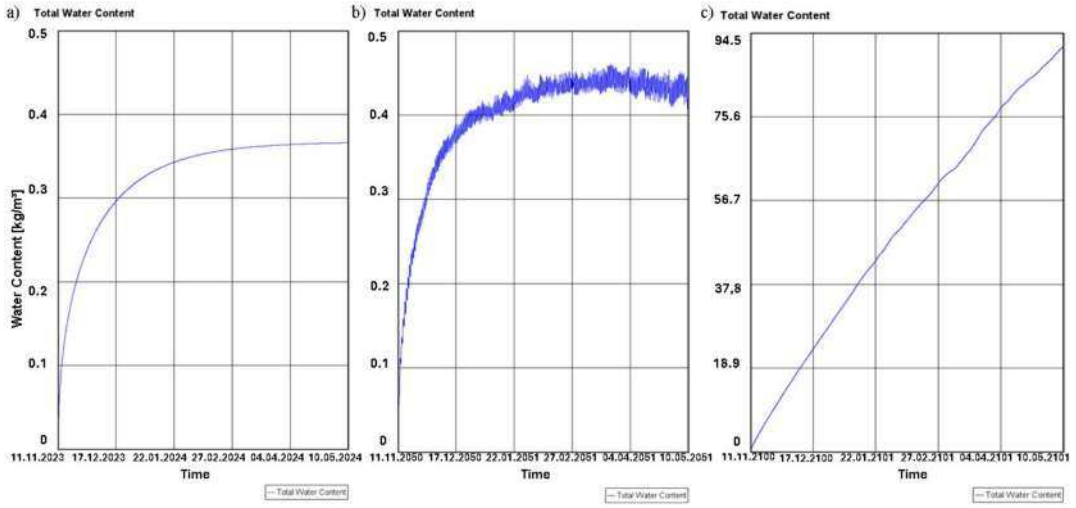

Fig. 18. Results of the simulation of rising damping behavior of historic masonries in terms of water content in 2023, 2050, and 2100.

for decision-making on interventions to mitigate the impact of climate warming in historical areas.

Mapping the environmental parameters of the Aracati historical center, the results demonstrate that the recovery materials and urban characteristics, such as buildings higher and volumetry, presence of green and free zones, conditioned the thermal behavior and the air quality. The path pavements recovered by stone and asphalt conduct the environment to a higher temperature than concrete pavements, while the presence of green areas reduces the temperature. Crossing information between urban data and environmental parameters can be a good way to understand microclimate behavior.

The street temperature mapping indicates a very concerning warming nowadays, with peaks of 39 °C during the day, while the concentration of CO_2 is also high (520 ppm). This environmental conduction can dramatically influence the life of the population that lives or visits the historic center. Considering the simulation for 2050 and 2100, the results indicated an increase in the temperature to 41 °C and 43 °C during the day. The findings also point to the morning and night becoming hotter than nowadays.

The simulation results indicate a dramatic scenario of historic masonry degradation. By the stress analysis, it was possible to observe a variation between 1.4814×10^{-12} MPa in 2023, to 1.544 MPa in 2050 till the maximum of 3.676 MPa in 2100, indicating a generalized presence of cracks in the masonries. Together with the existing load, it accelerates the mechanical failure of the masonry. The rising damping is also accelerated by temperature increase and the capillarity evolution to cracks formation, contributing to the layers decaying and the masonry degradation.

The results also demonstrate that the combination of multiparameter environmental data, urban information, and numerical simulations can be an assertive way to qualitatively evaluate the effects of climatic changes on cultural heritage. Furthermore, the information provided by the applicability of the presented methodology can support interventions and optimize the mitigation action on historic centers.

CRediT authorship contribution statement

Vitoria R.F. Pinheiro: Writing – original draft, Software, Investigation, Formal analysis. **Rafael Fontenele:** Writing – original draft, Software, Investigation, Data curation. **Allan Magalhães:** Writing – original draft, Software, Methodology, Investigation, Formal analysis, Data curation. **Naggila Frota:** Writing – review & editing, Visualization, Supervision, Methodology, Formal analysis, Data curation, Conceptualization. **Esequiel Mesquita:** Writing – review & editing, Visualization, Supervision, Resources, Project administration, Methodology, Formal analysis, Conceptualization.

Declaration of competing interest

The authors declare the following financial interests/personal relationships which may be considered as potential competing interests: Esequiel Mesquita reports financial support was provided by Coordination of Higher Education Personnel Improvement. Esequiel Mesquita reports financial support was provided by National Council for Scientific and Technological Development. Vitoria R. F. Pinheiro reports financial support was provided by Foundation for Scientific and Technological Development and Support of Ceará. If there are other authors, they declare that they have no known competing financial interests or personal relationships that could have appeared to influence the work reported in this paper.

Data availability

Data will be made available on request.

Acknowledgments

All authors acknowledge the Instituto do Patrimônio Histórico e Artístico Nacional (IPHAN) by technical support. The authors thank the Laboratory of Rehabilitation and Durability of Constructions (LAREB) for the support in the characterization tests. The authors also thank the Fraunhofer Institute for Building Physics for making the WUFIˆ® software available during the simulation period performed. The authors acknowledge the FUNCAP (01172921/2022) through financial support under the scope of the Scientist Chief Program: Culture and the Secretary of Culture of Ceará (SECULT). Esequiel Mesquita acknowledges CAPES and CNPQ – Project 302054/2022-7.

References

[1] D. Mitchell, C. Heaviside, S. Vardoulakis, C. Huntingford, G. Masato, B.P. Guillod, P. Frumhoff, A. Bowery, D. Wallom, M. Allen, Attributing human mortality during extreme heat waves to anthropogenic climate change, Environmental Research Letters 11 (2016), https://doi.org/10.1088/1748-9326/11/7/074006.
[2] G. Aktürk, A systematic overview of the barriers to building climate adaptation of cultural and natural heritage sites in polar regions, Environ Sci, Policy 136 (2022) 19–32, https://doi.org/10.1016/j.envsci.2022.05.016.
[3] Meehl Gerald A, Tebaldi Claudia, More intense, more frequent, and longer lasting heat waves in the 21st century, (2004).
[4] IPCC, IPCC Report 2022, International Panel on Climate Change (2022).

[5] Munich Re, Flood risk: Underestimated natural hazards, Https://Www.Munichre.Com/En/Risks/Natural-Disasters-Losses-Are-Trending-Upwards/Floods-and-Flash-Floods-Underestimated-Natural-Hazards.Html 1/688 online (2023).

[6] G. Nearing, D. Cohen, V. Dube, M. Gauch, O. Gilon, S. Harrigan, A. Hassidim, D. Klotz, F. Kratzert, A. Metzger, S. Nevo, F. Pappenberger, C. Prudhomme, G. Shalev, S. Shenzis, T.Y. Tekalign, D. Weitzner, Y. Matias, Global prediction of extreme floods in ungauged watersheds, Nature 627 (2024) 559–563, https://doi.org/10.1038/s41586-024-07145-1.

[7] J. Dong, Y. Schwartz, I. Korolija, D. Mumovic, The impact of climate change on cognitive performance of children in English school stock: A simulation study, Build Environ 243 (2023), https://doi.org/10.1016/j.buildenv.2023.110607.

[8] K. Bamdad, M.E. Cholette, S. Omrani, J. Bell, Future energy-optimised buildings — Addressing the impact of climate change on buildings, Energy Build 231 (2021), https://doi.org/10.1016/j.enbuild.2020.110610.

[9] I. Pigliautile, A.L. Pisello, A new wearable monitoring system for investigating pedestrians' environmental conditions: Development of the experimental tool and start-up findings, Science of the Total Environment 630 (2018) 690–706, https://doi.org/10.1016/j.scitotenv.2018.02.208.

[10] A.L. Pisello, A. Petrozzi, V.L. Castaldo, F. Cotana, On an innovative integrated technique for energy refurbishment of historical buildings: Thermal-energy, economic and environmental analysis of a case study, Appl Energy 162 (2014) 1313–1322, https://doi.org/10.1016/j.apenergy.2015.05.061.

[11] Howard L., The Climate of London - The Climate of London, (1833).

[12] OKE T. R., City size and the urban heat island, (1973).

[13] A.J. Arnfield, Two decades of urban climate research: A review of turbulence, exchanges of energy and water, and the urban heat island, International Journal of Climatology 23 (2003) 1–26, https://doi.org/10.1002/joc.859.

[14] I. Agathangelidis, C. Cartalis, M. Santamouris, Integrating urban form, function, and energy fluxes in a heat exposure indicator in view of intra-urban heat island assessment and climate change adaptation, Climate 7 (2019), https://doi.org/10.3390/cli7060075.

[15] M. Santamouris, L. Ding, F. Fiorito, P. Oldfield, P. Osmond, R. Paolini, D. Prasad, A. Synnefa, Passive and active cooling for the outdoor built environment – Analysis and assessment of the cooling potential of mitigation technologies using performance data from 220 large scale projects, Solar Energy 154 (2017) 14–33, https://doi.org/10.1016/j.solener.2016.12.006.

[16] R. Paolini, A. Zani, M. MeshkinKiya, V.L. Castaldo, A.L. Pisello, F. Antretter, T. Poli, F. Cotana, The hygrothermal performance of residential buildings at urban and rural sites: Sensible and latent energy loads and indoor environmental conditions, Energy Build 152 (2017) 792–803, https://doi.org/10.1016/j.enbuild.2016.11.018.

[17] M. Masoudi, P.Y. Tan, Multi-year comparison of the effects of spatial pattern of urban green spaces on urban land surface temperature, Landsc Urban Plan 184 (2019) 44–58, https://doi.org/10.1016/j.landurbplan.2018.10.023.

[18] H. Gilbert, B.H. Mandel, R. Levinson, Keeping California cool: Recent cool community developments, Energy Build 114 (2016) 20–26, https://doi.org/10.1016/j.enbuild.2015.06.023.

[19] M. Santamouris, On the energy impact of urban heat island and global warming on buildings, Energy Build 82 (2014) 100–113, https://doi.org/10.1016/j.enbuild.2014.07.022.

[20] S.E. Perkins, L.V. Alexander, J.R. Nairn, Increasing frequency, intensity and duration of observed global heatwaves and warm spells, Geophys Res Lett 39 (2012), https://doi.org/10.1029/2012GL053361.

[21] Dan Li, Elie Bou-Zeid, Synergistic Interactions between Urban Heat Islands and Heat Waves The Impact in Cities Is Larger than the Sum of Its Parts, (2013).

[22] I. Livada, A. Synnefa, S. Haddad, R. Paolini, S. Garshasbi, G. Ulpiani, F. Fiorito, K. Vassilakopoulou, P. Osmond, M. Santamouris, Time series analysis of ambient air-temperature during the period 1970–2016 over Sydney, Australia, Science of the Total Environment 648 (2019) 1627–1638, https://doi.org/10.1016/j.scitotenv.2018.08.144.

[23] Ł. Bratasz, R. Kozłowski, Ł. Bratasz, R. Kozłowski, Entwicklung der neuen EU-Normen-The CEN TC346 draft standard on heating historic churches: minimising disturbance to the indoor climate The CEN TC346 draft standard on heating historic churches: minimising disturbance to the indoor climate, 2007.

[24] D. Camuffo, E. Pagan, A. Bernardi, F. Becherini, The impact of heating, lighting and people in re-using historical buildings: A case study, J Cult Herit 5 (2004) 409–416, https://doi.org/10.1016/j.culher.2004.01.005.

[25] M.J. Varas-Muriel, R. Fort, Microclimatic monitoring in an historic church fitted with modern heating: implications for the preventive conservation of its cultural heritage, Build Environ 145 (2018) 290–307, https://doi.org/10.1016/j.buildenv.2018.08.060.

[26] D. Camuffo, E. Pagan, S. Rissanen, Ł. Bratasz, R. Kozłowski, M. Camuffo, A. della Valle, An advanced church heating system favourable to artworks: a contribution to European standardisation, J Cult Herit 11 (2010) 205–219, https://doi.org/10.1016/j.culher.2009.02.008.

[27] M.J. Varas-Muriel, R. Fort, M. Gómez-Heras, Assessment of an underfloor heating system in a restored chapel: Balancing thermal comfort and historic heritage conservation, Energy Build 251 (2021), https://doi.org/10.1016/j.enbuild.2021.111361.

[28] G.B.A. Coelho, H. Entradas Silva, F.M.A. Henriques, Impact of climate change in cultural heritage: from energy consumption to artefacts' conservation and building rehabilitation, Energy Build 224 (2020), https://doi.org/10.1016/j.enbuild.2020.110250.

[29] H.E. Silva, G.B.A. Coelho, F.M.A. Henriques, Climate monitoring in World Heritage List buildings with low-cost data loggers: The case of the Jerónimos Monastery in Lisbon (Portugal), Journal of Building Engineering 28 (2020), https://doi.org/10.1016/j.jobe.2019.101029.

[30] L. Kotova, J. Leissner, M. Winkler, R. Kilian, S. Bichlmair, F. Antretter, J. Moßgraber, J. Reuter, T. Hellmund, K. Matheja, M. Rohde, U. Mikolajewicz, Making use of climate information for sustainable preservation of cultural heritage: applications to the KERES project, Herit Sci 11 (2023), https://doi.org/10.1186/s40494-022-00853-9.

[31] V.L. Castaldo, A.L. Pisello, I. Pigliautile, C. Piselli, F. Cotana, Microclimate and air quality investigation in historic hilly urban areas: Experimental and numerical investigation in central Italy, Sustain Cities Soc 33 (2017) 27–44, https://doi.org/10.1016/j.scs.2017.05.017.

[32] L. Bencs, Z. Spolnik, D. Limpens-Neilen, H.L. Schellen, B.A.H.G. Jütte, R. Van Grieken, Comparison of hot-air and low-radiant pew heating systems on the distribution and transport of gaseous air pollutants in the mountain church of Rocca Pietore from artwork conservation points of view, J Cult Herit 8 (2007) 264–271, https://doi.org/10.1016/j.culher.2007.05.001.

[33] S. Bichlmair, R. Kilian, ROOM CLIMATE IN LINDERHOF PALACE Impact of ambient climate and visitors on room climate with a special focus on the bedchamber of King Ludwig II, 2010.

[34] R. Freeman, M. Yearworth, Climate change and cities: problem structuring methods and critical perspectives on low-carbon districts, Energy Res Soc Sci 25 (2017) 48–64, https://doi.org/10.1016/j.erss.2016.11.009.

[35] A.L. Pisello, Thermal-energy analysis of roof cool clay tiles for application in historic buildings and cities, Sustain Cities Soc 19 (2015) 271–280, https://doi.org/10.1016/j.scs.2015.03.003.

[36] G.B.A. Coelho, F.M.A. Henriques, Performance of passive retrofit measures for historic buildings that house artefacts viable for future conditions, Sustain Cities Soc 71 (2021), https://doi.org/10.1016/j.scs.2021.102982.

[37] L. Jiang, E. Lucchi, D. Del Curto, Adaptive reuse and energy transition of built heritage and historic gardens: The sustainable conservation of Casa Jelinek in Trieste (Italy), Sustain Cities Soc 97 (2023), https://doi.org/10.1016/j.scs.2023.104767.

[38] M. Santamouris, Cooling the cities - A review of reflective and green roof mitigation technologies to fight heat island and improve comfort in urban environments, Solar Energy 103 (2014) 682–703, https://doi.org/10.1016/j.solener.2012.07.003.

[39] F. Rossi, F. Cotana, M. Filipponi, A. Nicolini, S. Menon, A. Rosenfeld, Cool roofs as a strategy to tackle global warming: economical and technical opportunities, Advances in Building Energy Research 7 (2013) 254–268, https://doi.org/10.1080/17512549.2013.865555.

[40] Arthur H. Rosenfeld, Hashem Akbari, Joseph J. Romm, Melvin Pomerantz, Cool communities strategies for heat island mitigation and smog reduction, (1998).

[41] A.L. Pisello, E. Fortunati, C. Fabiani, S. Mattioli, F. Dominici, L. Torre, L.F. Cabeza, F. Cotana, PCM for improving polyurethane-based cool roof membranes durability, Solar Energy Materials and Solar Cells 160 (2017) 34–42, https://doi.org/10.1016/j.solmat.2016.09.036.

[42] A. de Gracia, L. Navarro, J. Coma, S. Serrano, J. Romaní, G. Pérez, L.F. Cabeza, Experimental set-up for testing active and passive systems for energy savings in buildings – Lessons learnt, Renewable and Sustainable Energy Reviews 82 (2018) 1014–1026, https://doi.org/10.1016/j.rser.2017.09.109.

[43] J. Coma, G. Pérez, A. de Gracia, S. Burés, M. Urrestarazu, L.F. Cabeza, Vertical greenery systems for energy savings in buildings: A comparative study between green walls and green facades, Build Environ 111 (2017) 228–237, https://doi.org/10.1016/j.buildenv.2016.11.014.

[44] G. Pérez, J. Coma, S. Sol, L.F. Cabeza, Green facade for energy savings in buildings: The influence of leaf area index and facade orientation on the shadow effect, Appl Energy 187 (2017) 424–437, https://doi.org/10.1016/j.apenergy.2016.11.055.

[45] M.F. Shahidan, P.J. Jones, J. Gwilliam, E. Salleh, An evaluation of outdoor and building environment cooling achieved through combination modification of trees with ground materials, Build Environ 58 (2012) 245–257, https://doi.org/10.1016/j.buildenv.2012.07.012.

[46] L. Quesada-Ganuza, L. Garmendia, I. Alvarez, E. Roji, Vulnerability assessment and categorization against heat waves for the Bilbao historic area, Sustain Cities Soc 98 (2023), https://doi.org/10.1016/j.scs.2023.104805.

[47] ICOMOS, The Venice charter for the conservation and restoration of monuments and sites., Venice, 1964.

[48] G. Leijonhufvud, A. Henning, Rethinking indoor climate control in historic buildings: The importance of negotiated priorities and discursive hegemony at a Swedish museum, Energy Res, Soc Sci 4 (2014) 117–123, https://doi.org/10.1016/j.erss.2014.10.005.

[49] B. Pioppi, I. Pigliautile, C. Piselli, A.L. Pisello, Cultural heritage microclimate change: Human-centric approach to experimentally investigate intra-urban overheating and numerically assess foreseen future scenarios impact, Science of the Total Environment 703 (2020), https://doi.org/10.1016/j.scitotenv.2019.134448.

[50] R.A.F. Oliveira, J. Lopes, H. Sousa, M.I. Abreu, A system for the management of old building retrofit projects in historical centres: the case of Portugal, International Journal of Strategic Property Management 21 (2017) 199–211, https://doi.org/10.3846/1648715X.2016.1251984.

[51] E. Mesquita, R. Martini, A. Alves, L. Mota, T. Rubens, P. Antunes, H. Varum, Heterogeneity detection of Portuguese-Brazilian masonries through ultrasonic velocities measurements, J Civ Struct Health Monit (2018), https://doi.org/10.1007/s13349-018-0312-5.

[52] L.M. Gomes de Oliveira, F. Lucas de Oliveira Freire, F.R. Carneiro Ribeiro, I.N.L. Sousa, E. Mesquita, A.A. Bertini, Investigation of the mortars and clay bricks of a luso-brazilian historic structure from XVIII century: The Nosso Senhor do Bonfim

Church, Journal of Building Engineering 45 (2022) 103592. doi: 10.1016/j.jobe.2021.103592.
[53] H.M. Künzel, Simultaneous heat and moisture transport in building components. One-and two-dimensional calculation using simple parameters: one- and two-dimensional calculation using simple parameters, IRB-Verlag Stuttgart 65 (1995) 65 p.
[54] K. Calvin, D. Dasgupta, G. Krinner, A. Mukherji, P.W. Thorne, C. Trisos, J. Romero, P. Aldunce, K. Barrett, G. Blanco, W.W.L. Cheung, S. Connors, F. Denton, A. Diongue-Niang, D. Dodman, M. Garschagen, O. Geden, B. Hayward, C. Jones, F. Jotzo, T. Krug, R. Lasco, Y.-Y. Lee, V. Masson-Delmotte, M. Meinshausen, K. Mintenbeck, A. Mokssit, F.E.L. Otto, M. Pathak, A. Pirani, E. Poloczanska, H.-O. Pörtner, A. Revi, D.C. Roberts, J. Roy, A.C. Ruane, J. Skea, P.R. Shukla, R. Slade, A. Slangen, Y. Sokona, A.A. Sörensson, M. Tignor, D. van Vuuren, Y.-M. Wei, H. Winkler, P. Zhai, Z. Zommers, J.-C. Hourcade, F.X. Johnson, S. Pachauri, N.P. Simpson, C. Singh, A. Thomas, E. Totin, A. Alegría, K. Armour, B. Bednar-Friedl, K. Blok, G. Cissé, F. Dentener, S. Eriksen, E. Fischer, G. Garner, C. Guivarch, M. Haasnoot, G. Hansen, M. Hauser, E. Hawkins, T. Hermans, R. Kopp, N. Leprince-Ringuet, J. Lewis, D. Ley, C. Ludden, L. Niamir, Z. Nicholls, S. Some, S. Szopa, B. Trewin, K.-I. van der Wijst, G. Winter, M. Witting, A. Birt, M. Ha, IPCC, 2023: Climate Change 2023: Synthesis Report. Contribution of Working Groups I, II and III to the Sixth Assessment Report of the Intergovernmental Panel on Climate Change [Core Writing Team, H. Lee and J. Romero (eds.)]. IPCC, Geneva, Switzerland., 2023. doi: 10.59327/IPCC/AR6-9789291691647.
[55] NTC, Norme tecniche per le costruzioni. DM 17/1/2018, Gazzetta Ufficiale Della Repubblica Italiana 20 (2018).
[56] F. Brandão, A. Diógenes, J. Fernandes, E. Mesquita, M. Betti, Seismic behavior assessment of a brazilian heritage construction, Frattura Ed Integrita Strutturale 12 (2018), https://doi.org/10.3221/IGF-ESIS.45.02.
[57] F. Brandão, E. Mesquita, A. Diógenes, P. Antunes, H. Varum, Dynamic characterization of a heritage construction from 19th century, Revista IBRACON De Estruturas e Materiais 11 (2018) 52–75, https://doi.org/10.1590/s1983-41952018000100004.
[58] .B. Lourenço, Computational strategies for masonry structures, 1996. doi: ISBN 90-407-1221-2.
[59] J. Ortega, G. Vasconcelos, P.B. Lourenço, H. Rodrigues, H. Varum, Seismic behaviour assessment of vernacular isolated buildings, in: Correia, Lourenço, Varum (Eds.), Seismic Retrofitting: Learning from Vernacular Architecture, 1st ed., Taylor & Francis, London, 2015: pp. 203–212.
[60] I. Ministro, T. Con, G. Ufficiale, Circolare 2 febbraio 2009, n. 617, Verifiche (2009).
[61] Greven, H, Seele, J, Alvenarias afetadas por umidade e sais, 2022. 1 ed. LEUD Editora, São Paulo.
[62] C.Y. Yiu, D.C.W. Ho, S.M. Lo, Weathering effects on external wall tiling systems, Constr Build Mater 21 (2007), https://doi.org/10.1016/j.conbuildmat.2005.11.002.
[63] Ana Gabriela Saraiva, Contribuição ao estudo de tensões de natureza térmica em sistemas de revestimento cerâmico de fachada, University of Brasilia, 1998.
[64] J. Xiao, Z. Li, Q. Xie, L. Shen, Effect of strain rate on compressive behaviour of high-strength concrete after exposure to elevated temperatures, Fire Saf J 83 (2016), https://doi.org/10.1016/j.firesaf.2016.04.006.
[65] Z.P. Bažant, G. Cusatis, L. Cedolin, Temperature effect on concrete creep modeled by microprestress-solidification theory, J Eng Mech 130 (2004), https://doi.org/10.1061/(asce)0733-9399(2004)130:6(691).
[66] J.A. Sainz-Aja, I.A. Carrascal, J.A. Polanco, C. Thomas, Effect of temperature on fatigue behaviour of self-compacting recycled aggregate concrete, Cem Concr Compos 125 (2022), https://doi.org/10.1016/j.cemconcomp.2021.104309.